Triplet State and Dynamics of Photoexcited C_{70}

Haim Levanon,* Vladimir Meiklyar, Shalom Michaeli, and Dan Gamliel

Contribution from the Department of Physical Chemistry and The Farkas Center for Light-Induced Processes, The Hebrew University of Jerusalem, Jerusalem 91904, Israel

*Received February 1, 1993**

Abstract: The photoexcited triplet of C_{70}, in toluene, was investigated by time-resolved EPR spectroscopy. Over the entire range of temperatures (8–213 K) the resulting early-time signal is attributed to the polarized EPR triplet spectrum, which evolves in time into a thermalized spectrum. Similar to the case of $^3C_{60}$, the narrow liquid-phase spectrum is due to rotational narrowing of the thermal triplet. At both low and high temperatures the results indicate the coexistence of two triplets, differing greatly in their relaxation rates.

Introduction

The detection of the photoexcited triplet state of C_{60} and C_{70} by EPR stimulated a series of investigations focused on the determination of the magnetic parameters and dynamics of this paramagnetic state.[1] Although all reports agree that the low-temperature spectra are associated with the photoexcited triplet, the assignment of the high-temperature spectra of C_{60} following light excitation is still ambiguous. When C_{60} or C_{70} is dissolved in a glass or amorphous matrix, at low temperatures, it was found that their triplet dynamics are governed by pseudorotation, i.e., jumps between Jahn–Teller (JT) states which are apparently very close in energy.[1g,k] In the case of $^3C_{60}$, the two-site exchange model was found to describe quite accurately the details of the triplet line shape, whereas the model of ordinary rotational diffusion was unable to account for EPR spectra. At higher temperatures, when the solvent was in the liquid phase, the reverse was found to be true. The exchange model was not satisfactory, and the assumption of Brownian rotational diffusion gave a good fit to the experimental line shapes.[1g] The conclusion that fast molecular rotation is present at high temperatures is consistent with that suggested first by Closs et al.[1c] On the other hand, a recent report claims that the narrow liquid-phase spectra should be ascribed to the doublet state, i.e., the radical anion, $C_{60}^{\bullet-}$.[1h] We believe that the evidence for a fast-rotating triplet as the origin of the unusually narrow EPR line in the case of C_{60} is reliable in itself.[1c,g,j] Nevertheless, in the present study, we provide independent indirect evidence to the same point, by presenting data on the photoexcited triplet state of C_{70}, randomly oriented in toluene. We also find, over the entire range of temperatures, clear evidence for the simultaneous presence of two triplets, one of which decays much faster than the other, as will be discussed below.

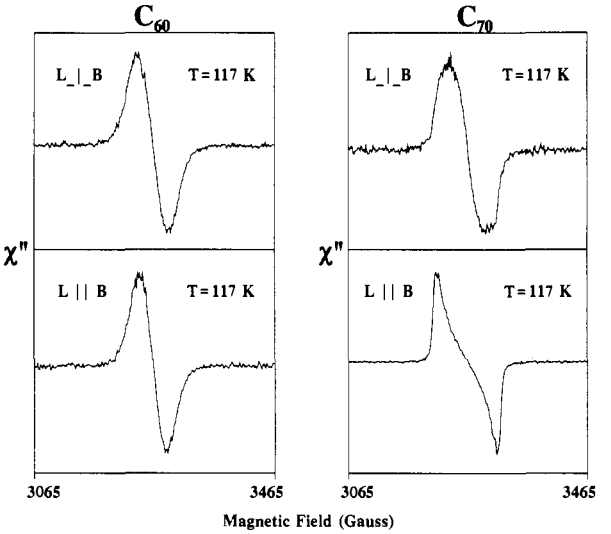

Figure 1. Direct detection triplet EPR spectra of C_{60} and C_{70} in a frozen nematic liquid crystal ($E-7$) in the parallel and perpendicular orientations. All spectra were taken at 300 ns after the laser pulse (λ_{exc} = 532 nm, 20–25 mJ/pulse), microwave power 40 mW, concentration $\sim 5 \times 10^{-4}$ M. For details see ref 1d,g.

Experimental Section

Two modes of time-resolved CW-EPR methods were utilized to detect the photoexcited paramagnetic states, i.e., laser excitation and time-resolved direct detection (DD)[2] and light-modulation field-modulation (LFM) EPR detection.[3] EPR samples were prepared by dissolving purified C_{70}[4] in either isotropic (toluene) or anisotropic (a nematic liquid crystal, LC) medium. All samples (2×10^{-5} to 5×10^{-3} M), before and after being photoexcited, were checked for their optical absorption spectra.[5] The details of the experimental methods are described extensively in a very recent publication.[1g]

Results and Discussion

Experimental Results. The basic difference between the symmetries of C_{60} and C_{70} in their photoexcited triplet states is best manifested by the triplet spectra taken with the LC as a solvent (Figure 1). One immediately notices the clear dependence of the spectra on the orientation of the director, **L**, relative to the external magnetic field, **B**. Such an orientation dependence is

* Abstract published in *Advance ACS Abstracts*, August 15, 1993.

(1) (a) Wasielewski, M. R.; O'Neil, M. P.; Lykke, K. R.; Pellin, M. J.; Gruen, D. M. *J. Am. Chem. Soc.* **1991**, *113*, 2774. (b) Lane, P. A.; Swanson, L. S.; Ni, O.-X.; Shinar, J.; Engel, J. P.; Barton, T. J.; Jones, L. *Phys. Rev. Lett.* **1991**, *68*, 887. (c) Closs, G. L.; Gautam, P.; Zhang, D.; Krusic, P. J.; Hill, S. A.; Wasserman, E. *J. Phys. Chem.* **1992**, *96*, 5228. (d) Levanon, H.; Meiklyar, V.; Michaeli, A.; Michaeli, S.; Regev, A. *J. Phys. Chem.* **1992**, *96*, 6128. (e) Terazima, M.; Hirota, N.; Shinohara, H.; Saito, Y. *Chem. Phys. Lett.* **1992**, *195*, 333. (f) Groenen, E. J. J.; Poluektov, O. G.; Matsushita, M.; Schmidt, J.; van der Waals, J. H. *Chem. Phys. Lett.* **1992**, *197*, 314. (g) Regev, A.; Gamliel, D.; Meiklyar, V.; Michaeli, S.; Levanon, H. *J. Phys. Chem.* **1993**, *97*, 3671. (h) Ruebsam, M.; Dinse, K.-P.; Plueschau, M.; Fink, J.; Krätschmer, W.; Fostiropoulos, K.; Taliani, C. *J. Am. Chem. Soc.* **1992**, *114*, 10059. (i) A different model, suggesting superposition of two triplets in frozen benzonitrile, has been reported recently: Bennati, M.; Grupp, A.; Mehring, M.; Dinse, K.-P.; Fink, J. *Chem. Phys. Lett.* **1992**, *200*, 440. (j) Zhang, D.; Norris, J. R.; Krusic, P. J.; Wasserman, E.; Chen, C. C.; Lieber, C. M. Preprint, submitted to *J. Phys. Chem.* (k) Terazima, M.; Sakurada, K.; Hirota, N.; Shinohara, H.; Saito, Y. Preprint.

(2) Gonen, O.; Levanon, H. *J. Chem. Phys.* **1986**, *84*, 4132.

(3) Levanon, H.; Vega, S. *J. Chem. Phys.* **1974**, *61*, 2265.

(4) Parker, D. H.; Wurz, P.; Chatterjee, K.; Lykke, K. R.; Hunt, J. E.; Pellin, M. J.; Hemminger, J. C.; Gruen, D. M.; Stock, L. M. *J. Am. Chem. Soc.* **1991**, *113*, 7499.

(5) (a) Tanigaki, K.; Ebbesen, T. W.; Kuroshima, S. *Chem. Phys. Lett.* **1991**, *185*, 189. (b) Hare, J. P.; Kroto, H. W.; Taylor, R. *Chem. Phys. Lett.* **1991**, *177*, 394.

0002-7863/93/1515-8722$04.00/0 © 1993 American Chemical Society

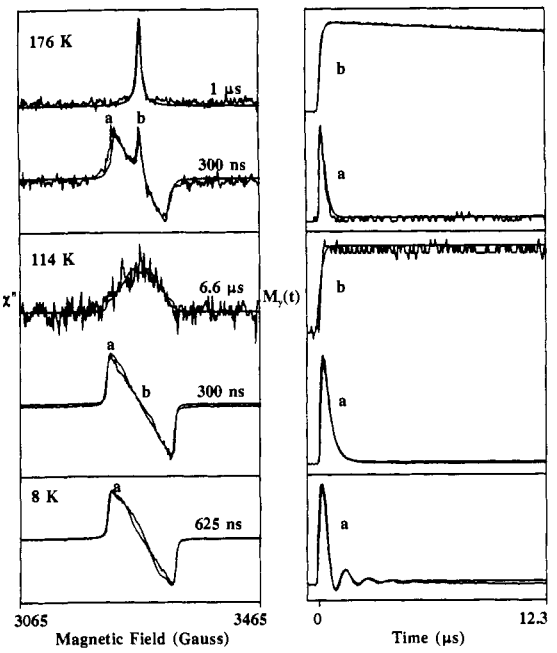

Figure 2. Time-resolved triplet DD-EPR spectra of C_{70} randomly oriented in toluene in the glass and amorphous phases as a function of temperature (λ_{exc} = 532 nm, 20–25 mJ/pulse, microwave power 40 mW, concentration $\sim 10^{-4}$ M). The spectrum at 8 K was taken at a delay of 625 ns after the laser pulse; the other spectra were taken at delays of 300 ns, 6.6 μs, and 1.0 μs. The smooth lines superimposed on the spectra are the simulated curves: at 8 and 114 K the simulations refer to one polarized triplet undergoing discrete jumps; at 176 K the simulation refers to a 1:1 ratio of polarized and thermalized triplets. The latter triplet undergoes rotational motion at a rate of $1/\tau_R = 1.5 \times 10^9$ s^{-1} and $1/T_2 = 2$ G. The corresponding temporal behaviors of the magnetization curves, $M_y(t)$, are presented on the right. The "a" and "b" marks are the field positions where the kinetics were taken. The smooth lines are the simulated curves: at 8 K the simulation of the kinetics consists of two triplets with $T_1(1) = 5.0$ μs, $T_2(1) = 0.5$ μs and $T_1(2) = 0.6$ μs, $T_2(2) = 0.1$ μs, with weighting factors 1:5, respectively; at 114 and 176 K the simulations consist of one triplet only (see text).

not found in C_{60}, where spectra taken at parallel and perpendicular orientations were identical.[1d,g] This difference in spectral behavior obviously results from the elongated shape of C_{70}, which causes it to align preferentially parallel to the liquid crystalline director, **L**, in contrast to the roughly spherical C_{60} molecules, which do not have such a preferred alignment.

To understand the dynamic behavior associated with $^3C_{70}$ in an isotropic environment (toluene), we have measured the triplet spectra over a wide range of temperatures, according to the phase transitions scheme of toluene:[1d,6]

$$8\ \text{K} \xrightarrow{\text{glass}} 117\ \text{K} \xrightarrow{\text{amorphous}} 178\ \text{K} \xrightarrow{\text{liquid}} \quad (1)$$

Inspection of the early-time broad spectra (Figure 2) at 8, 114, and 176 K indicates immediately that, unlike the case of C_{60}, the line shape variations with temperature are very small. In the case of C_{60}, the temperature dependence was explained by pseudorotation, i.e., exchange between degenerate Jahn–Teller configurations, associated with the x and z components of the zero field splitting (ZFS) tensor.[1c,g,7] Under such a mechanism, the spectral width should be strongly dependent upon the rotation rate. In the case of $^3C_{70}$, two possibilities may account for the small changes of the triplet spectra in this range of temperatures: (1) lack of dynamics associated with $^3C_{70}$ at temperatures where the rigidity of the solvent may prohibit molecular rotation; (2) triplet dynamics is maintained via the long axis (z) of the ZFS tensor. As will be shown below, the first alternative is ruled out on the basis of line-shape analysis. The sharp spectrum superimposed on the broad early-time spectrum (Figure 2, top) will be discussed separately.

The early-time spectra characterize the photoexcited triplet, $^3C_{70}$, born in a non-Boltzmann distribution (spin polarization), and are in agreement with those reported recently.[1e,k] However, the time-evolved spectra exhibit noticeable changes of the spectral features, where the absorption/emission pattern at early-time changes into an absorption mode at later times. The half-width of the absorption spectrum coincides with the peak-to-peak distance of the polarized one, indicating the common origin of both spectra, namely the triplet state. The kinetic curves of the magnetization behavior, $M_y(t)$, taken at two different field positions, are also shown in Figure 2. The transient kinetics taken at field position a is related to the polarized triplet, whereas the long-lived kinetics taken at field position b is related to the absorption spectrum. Evidently, the broad absorption should be attributed to the thermalized triplet with a Boltzmann distribution of the triplet sublevels population. The absence of a late-time absorption spectrum at 8 K in Figure 2 is due to the persistence of polarized triplet spectra over a wide time scale as a result of long spin lattice relaxation time, preventing a reasonable detection of an absorption spectrum. Moreover, the spectral changes in time that occur in the polarized triplet spectra are described by Terazima et al.[1k] and will not be treated in this work.

The results summarized above indicate that, at the temperature region below the transition state from amorphous to liquid toluene (at 178 K), both the spectral and the kinetic behavior (not shown) do not change. However, on approaching the transition state, a sharp feature starts to grow at the center of the polarized spectrum (Figure 2, top). Again, similar to the low-temperature spectra, the early-time broad spectrum is the polarized triplet, and the superimposed narrow spectrum, as well as the later time spectrum, appears in an absorption mode. Finally, above the phase-transition temperature, in the liquid phase, only a narrow sharp spectrum is observed (Figure 3). The kinetics associated with the narrow spectra at 176 and 213 K also confirm the absorptive nature of these spectra. In addition to the DD-EPR measurements, an LFM-EPR spectrum was also taken at 213 K (Figure 3). Whereas the DD-EPR spectrum is structureless, probably because of a poor signal-to-noise ratio, the spectrum taken under LFM conditions consists of a doublet, superimposed on a broad spectrum, which appears to be absorptive. However, even this broad component is much narrower than that in the low-temperature spectra. Numerical integration of the LFM-EPR spectrum results in a spectrum which is practically identical to that observed in the DD method (Figure 3).

The experimental observations described above can be divided into two regimes: (1) temperatures below the phase transition (178 K), in the solid phase; and (2) temperatures above the phase transition, in the liquid phase. Thus the dynamics of $^3C_{70}$ will also be treated accordingly. The resemblance between the triplet spectra of $^3C_{70}$ and $^3C_{60}$ (in particular in the liquid phase) will guide us in the quantitative analysis, similar to that carried out with $^3C_{60}$.[1g]

Triplet Dynamics via Line-Shape Analysis. For a coherent presentation we outline below the basic considerations of the triplet line-shape analysis. The symmetry of C_{70} in the ground state is D_{5h}, so we suggest that the molecule in its excited triplet state has some stable sites in a rigid matrix.[1g,7,8] The dynamics of $^3C_{70}$ in frozen toluene is then pseudorotation, i.e., discrete reorientation of the spin hamiltonian in the molecular-fixed frame of reference. Thus, the hopping process can be described by intramolecular

(6) Alba, C.; Busse, L. E.; List, D. J.; Angell, C. A. *J. Chem. Phys.* **1990**, *92*, 617.

(7) (a) Bersuker, I. B. *The Jahn-Teller Effect and Vibronic Interaction in Modern Chemistry*; Plenum Press: New York, 1984; pp 82–91. (b) Negri, F.; Orlandi, G.; Zerbetto, F. *Chem. Phys. Lett.* **1988**, *144*, 31. (c) Koga, N.; Morokuma, K. *Chem. Phys. Lett.* **1992**, *196*, 191.

(8) Andreoni, W.; Gygi, F.; Parrinello, M. *Chem. Phys. Lett.* **1992**, *189*, 241.

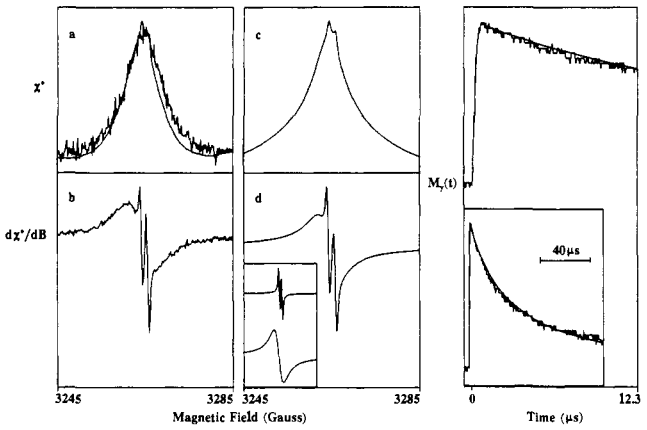

Figure 3. On the left: (a) comparison of a time-resolved DD-EPR spectrum of $^3C_{70}$, randomly oriented in toluene in the liquid phase, at a temperature of $T = 213$ K, with the numerical integration (smooth line) of the LFM-EPR spectrum appearing in part b of this figure; (b) LFM-EPR spectrum ($\lambda_{exc} > 400$ nm, field- and light-modulation frequency are 100 KHz and 500 Hz, respectively). Concentration and microwave power are as in Figure 2. The smaller of the two sharp peaks in the numerically integrated line in part a is partly hidden by the noisy DD-EPR spectrum. In the middle column, simulations of the (c) absorption (DD-EPR) and (d) derivative (LFM-EPR) spectra are presented. The spectra are sums of two components, calculated with a different width and resonance position (the derivatives are shown in the inset). The parameters used were $D = -0.00523$ cm^{-1}, $E = -0.00169$ cm^{-1} for both spectra, $1/T_2 = 0.1$ G for the narrow component, and $1/T_2 = 3.0$ G for the broad component, which has $\Delta g = 0.0006$ relative to the narrow component. The respective weighting factors taken in the simulation are 1:3.5 (for details see text). The corresponding temporal behavior of the magnetization $\mathbf{M}_y(t)$ is presented on the right-hand column for the DD-EPR spectrum over a period of 12.3 μs (top) and over a longer period (inset, bottom). The smooth curves were determined by using eqs 6 and 9.

exchange of the principal axes of the dipolar tensor, in terms of the density matrix formalism[1g]

$$\rho_{ij} = \rho_{ij}^{A,B} = \rho_{ij}^{A} + \rho_{ij}^{B} \quad (2)$$

where $\rho_{ij}^{A,B}$ describes the EPR transitions within the $\Delta M_s = \pm 1$ spectral range and A and B are the two sites between which the exchange takes place. In the discrete jump model, the line shape should depend on the hopping rate, k_{HOP}, and the correlation time for such a process is $\tau_{HOP} = 1/k_{HOP}$. The relation between the two principal axes systems of the two sites is expressed by the Euler rotation matrix. The dynamics is inserted into the expression for static randomly oriented triplets, given by[1g]

$$\chi''(\mathbf{B},t) \propto \sum_{\substack{i=1,2 \\ j=i+1}} \int_0^{\pi/2} \int_0^{\pi/2} \mathrm{Im}[\rho_{ij}(\theta,\phi,t)]\mathbf{M}(\theta,\phi) \quad (3)$$

where $\rho_{ij}(\theta,\phi,t)$ is the density matrix element connecting the i,j levels with θ and ϕ as the angles of external magnetic field $\mathbf{B}$ in the principal axes system of reference, $M(\theta,\phi) = \sin\theta\, d\theta\, d\phi$ is the distribution function in the isotropic matrix, and the summation is over two possible EPR transitions. Within this model, it is possible to control the amplitude of the jumps and to sum over a range of different configurations.

Another possible model for molecular motion is that of Brownian rotational diffusion, due to actual rotations which are partly hindered by random molecular collisions. One may also treat in this approach some variations on the Brownian diffusion model. With rotational diffusion, the line shape is given by[1g,9]

$$\chi''(\omega) = -\omega \int_0^\infty \cos(\omega t) \sum_{m,n} \{((\rho_0)_{mm} - (\rho_0)_{nn})/(E_m - E_n)\}(\mathbf{S}_x(t))_{mn}(\mathbf{S}_x)_{nm}\, dt \quad (4)$$

assuming the photoexcitation process populated the triplet levels

(9) Gamliel, D.; Levanon, H. *J. Chem. Phys.* **1992**, *97*, 7140.

Table I. Magnetic and Dynamic Parameters of $^3C_{70}$ in Toluene

T (K)[a]	$1/\tau_{HOP}$[b]	D[c]	E[c]	A_x:A_y:A_z	T_1[d]	T_2[d]
8	1.7(±0.5)	−53	−6	0.06:1.0:0.1	5.0[e]	0.5[e]
114	3.4(±0.5)	−53	−6	0.06:1.0:0.1	0.6	0.1
176	5.0(±0.5)	−50	−5	0.06:1.0:0.1	0.25	0.1
213[f]		−52.3	−16.9	1.0:1.0:1.0	0.28	0.1

[a] ±0.5 K. [b] Determined via the discrete jumps model ($\times 10^7$ s^{-1}). [c] $\times 10^4$ cm^{-1}. Input parameters for simulations assuming $D, E < 0$. [d] In μs. Estimated error ±0.05 μs. [e] For the second triplet, $T_1 = 0.6$ μs and $T_2 = 0.1$ μs. [f] At this temperature $1/\tau_R$ determined via the diffusion rotation model is 1.8×10^9 s^{-1}, k_T determined via the discrete jumps model is $4(\pm 0.8) \times 10^3$ s^{-1}, and $2k_{TT}$ is $0.5(\pm 0.1) \times 10^9$ M^{-1} s^{-1}.

with no significant coherence between them. Here E_m is an energy level ($m = -1, 0, 1$ for a triplet) and terms with $E_m = E_n$ are excluded from the summation. ρ_0 is the initial density matrix immediately after the ISC transition to the triplet state, $\mathbf{S}_x$ is the magnetization operator, and $\mathbf{S}_x(t)$ is the time-dependent magnetization. The latter quantity is calculated by solving the stochastic Liouville equation (SLE) for the density matrix. The rotational diffusion rates R are related to the correlation time by $\tau_R = 1/6R$. If the rotation is highly anisotropic, one needs to calculate separate correlation times for the different rates. Assuming an axially symmetric diffusion tensor, one has $\tau_{R(\parallel)} = 1/6R_\parallel$ and $\tau_{R(\perp)} = 1/6R_\perp$, where the parallel direction refers to the symmetry axis of the diffusion tensor and the perpendicular direction refers to any direction in the plane perpendicular to that axis.

Low Temperature: Dynamics in the Rigid Phase. The left-hand side of Figure 2 shows the experimental line shape together with the simulated triplet spectra undergoing solid-like discrete jumps of 72° (±5) about the long dipolar axis z. The temperatures, the ZFS parameters (D and E), and rate of rotation are given in Table I and are in line with very recent results of Terazima et al.[1k] Notice that, similar to the case of $^3C_{60}$, a negative sign is assigned to D and, according to our assignment of the principal axes (see Appendiix), $E < 0$ as well. Unlike $^3C_{60}$, where the discrete jumps are between the x- (or y-) and z-axes (axis of rotation is y or x), in the present case the axis of rotation is z; that is consistent with the lower symmetry of C_{70}. Also, as noted in Table I, the variation of the rotation rates with temperature is not as conspicuous as in the case of C_{60}.[1g]

As mentioned earlier, the time-evolved spectra are reflected by the kinetics taken at different field positions. The expression for the magnetization, $\mathbf{M}_y(t)$, can be found from the general solution of the Bloch equations.[10] If the observation is on-resonance, the magnetization of a spin polarized triplet evolves as[10]

$$\mathbf{M}_y(t) = (\omega_1/b)e^{at} \sin bt \quad (5)$$

and the magnetization of a thermally equilibrated triplet evolves as

$$\mathbf{M}_y(t) = (\omega_1/T_1c)\{[(a/b) \sin bt - \cos bt]e^{at} + 1\} \quad (6)$$

In these equations the following definitions are used:

$$a = -{}^1/_2(T_2^{-1} + T_1^{-1}); b = [\omega_1^2 - {}^1/_4(T_2^{-1} - T_1^{-1})^2]^{1/2}; c = a^2 + b^2 \quad (7)$$

where ω_1 is the microwave power. If the irradiation is weak relative to the inverse decay constants, so that $\omega_1 < {}^1/_2(T_2^{-1} - T_1^{-1})$, then b in eq 7 is imaginary. Consequently, the sine and cosine functions in eqs 5 and 6 are a difference and a sum, respectively, of exponentials of real arguments. This is the case of overdamping, where the magnetization decays without any oscillations. In the opposite case, $\omega_1 > {}^1/_2(T_2^{-1} - T_1^{-1})$, the signal

(10) (a) Hore, P. J.; McLauchlan, K. A. *J. Magn. Reson.* **1979**, *36*, 129. (b) Hore, P. J.; McLauchlan, K. A. *Rev. Chem. Intermed.* **1979**, *3*, 89.

does oscillate, which corresponds to underdamping, giving rise to transient nutations (Torrey oscillations). For sufficiently high temperatures one has $T_1 = T_2$, and then eq 6 above is identical to the expression used for simulating the high-temperature kinetics of $^3C_{60}$. As in that case, the expression for $M_y(t)$ must be multiplied by an overall decay factor, as will be discussed below.

The Torrey oscillations that appear at 8 K could only be simulated by summing over the magnetization, calculated from eq 5, of two different polarized triplets. The two triplets have the same magnetic parameters and the same polarization, but one of them decays slowly (T_1 = 5.0 μs, T_2 = 0.5 μs) whereas the other one decays fast (T_1 = 0.6 μs, T_2 = 0.1 μs). The appearance of two polarized triplets in the kinetics was checked for several different values of ω_1 (only one of them is shown in Figure 2). The signal of the faster decaying triplet was multiplied by a factor of 5 (relative to the other signal) in order to get the best fit in the simulated kinetic curve. This summation of signals, with this relative strength factor, is consistent with results obtained for the liquid-phase spectrum (see below). In the intermediate-temperature range the kinetics are simply described by a single triplet, again using eq 5. The absence of a second triplet in that case is presumably due to the following reason. At very low temperatures the signals decay very slowly, so even the fast decaying component is not too fast to be detected. At intermediate temperatures the relaxation times are significantly shorter (almost by an order of magnitude), so the fast component has practically decayed to zero before the first point in the signal is measured. At high temperatures (in the liquid phase) the kinetics do not require more than one triplet, but the line shape is very narrow so the difference between the two triplets is manifested there. Finally, the spectra attributed to the thermalized triplet decay very slowly, corresponding to the slow decay of the triplet to the ground state.[11] The magnetic relaxation parameters used in the simulations, T_1 and T_2, are given in Table I.

High Temperature: Dynamics in the Liquid Phase. About the melting point, 176 K, two spectra are detected, i.e., a relatively broad a/e triplet (ΔH_{p-p} = 77 G) superimposed on a very narrow signal in an absorption mode (ΔH = 7 G). The simultaneous appearance of the two spectra is attributed to the solvent's transition state, where both the solid and liquid phases coexist (soft glass) giving rise to two types of spectra. At higher temperatures in the liquid phase, only the narrow signal superimposed on a broader spectrum is detected (cf. LFM spectrum in Figure 3). The appearance of a narrow spectrum above the melting point suggests immediately that $^3C_{70}$ undergoes a dynamical process responsible for strong motional narrowing as observed for $^3C_{60}$. The narrow line observed above the melting point is consistent with the model of fast rotational diffusion, as noted for the case of C_{60}.[1c,d,g] However, the dynamic mechanism which accounts for the narrow spectrum in the liquid phase indicates that the rotation is apparently not isotropic but seems to occur mainly about the x-axis, averaging partially the ZFS terms, D and E, in the y–z plane. This is best shown in Figure 4, where we apply the model of discrete jumps of 90° about the x-axis with different rotation rates and arbitrary ZFS parameters, e.g., D = –0.0053 and E = –0.0009 cm^{-1} (a similar result is obtained in the rotational diffusion model). Thus, the dynamics in the present case is associated with different axes of the ZFS tensor, compared with the low-temperature results.

According to this model, simulation of the high-temperature spectrum (T = 213 K) was carried out by considering two types of motions. The first is Brownian rotational diffusion, which is highly anisotropic, taking place effectively only about the x-axis. Such rotations were calculated by tilting the diffusion tensor axis system by θ = 90°, ϕ = 0° relative to the principal axis system (PAS) of the ZFS tensor. Thus, the main diffusion axis ("z"-axis) is the x-axis of the ZFS tensor. Rotation about other axes was assumed to be in the effective rigid limit regime ($R_\perp \leq 3 \times 10^5$ s^{-1}). Rotation about the main axis with a rate of about $R_\parallel = 3 \times 10^8$ s^{-1} (corresponding to a correlation time of $\tau_{R(\parallel)} \approx 6 \times 10^{-10}$ s^{-1}) gave a reasonable fit to the sharp features of the line shape. The broad spectral component was simulated with the same parameters except that the line width was changed from $1/T_2$ = 0.1 G to $1/T_2$ = 3 G and the center of the line was shifted by 1 G (Δg = 0.0006). The two components were scaled and added together, giving the broad component a weight of 3.5 relative to the weight of the other component. The broad component apparently comes from a second type of $^3C_{70}$ in which the line shape is inhomogeneously broadened. The appearance of two fullerene triplets is consistent with previous observations[1i] and predictions for C_{60}[7b,c] and possibly C_{70}.[8] The inhomogeneuos broadening of the second triplet is consistent with other results for C_{70}.[1k] The appearance of two triplets with very different line-width parameters is also consistent with the analysis of the kinetics at 8 K, as discussed above.

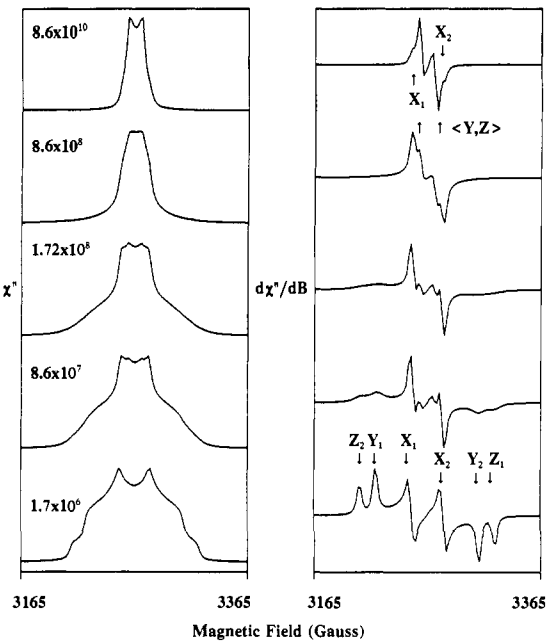

Figure 4. Simulated absorption (left) and derivative (right) line shapes of a thermalized model triplet with D = –0.0053 and E = –0.0009 cm^{-1}, undergoing discrete jumps (similar results are obtained with rotational diffusion) about the x axis at different rates, indicated in the figure (in s^{-1}). The arrows below indicate the canonical orientations of the nearly static triplet. The arrows on the top spectrum indicate the canonical orientation x and the motionally averaged y and z positions denoted by $\langle y,z \rangle$. The angular jumps were assumed to be of 90°, and the line-width parameter is $1/T_2$ = 2 G.

The second type of motion considered is large-amplitude jumps of 90° (pseudorotation) with the correlation times between $\tau_{HOP} = 10^{-11}$ s and $\tau_{HOP} = 5 \times 10^{-10}$ s. Also in this case, using the two-triplets assumption, a fairly good fit was achieved to the experimental line shape, almost of the same quality as with the rotational diffusion model.

Since both types of the motion can account in a similar manner for the line shape, there is no unambiguous proof that one kind of motion is dominant. However, considering the high temperature and the liquid phase of the solvent, we presume that the actual motion is rotational diffusion. This is consistent with results for C_{60}[1g] and for many other molecules observed in liquid solutions.[12]

An additional unique feature, not found in the case of $^3C_{60}$, is the variation of the ZFS term E, where the liquid-phase triplet could be best simulated with $D \approx 3E$ (Table I). Such a case

(11) In agreement with laser photolysis data on the triplet state of C_{70}, e.g.: (a) Arbogast, J. W.; Foote, C. S. *J. Am. Chem. Soc.* **1991**, *113*, 8886. (b) Dimitrijević, N. M.; Kamat, P. V. *J. Phys. Chem.* **1992**, *96*, 4811.

(12) Freed, J. H. In *Spin Labeling*; Berliner, L. J., Ed.; Academic Press: New York, 1976; Chapter 3, p 53.

corresponds to a large symmetry distortion, for which the sign of E should be the same as that of D, i.e., negative, if the axis of rotation is x, as assumed in the line-shape simulations (see Appendix).

Similar to the case of $^3C_{60}$, the slow decay of the narrow spectrum cannot be described by a polarized rotating triplet. It is conceivable that the fast spin relaxation in the liquid phase would have resulted in a detection of thermalized triplets (Figure 3, top). Moreover, the conclusion on $^3C_{70}$ with thermal spin equilibrium is in line with the relatively slow buildup and decay of the narrow absorption spectra (Figure 3). Simulations of the kinetic curves in the liquid phase were carried out by using the same model as was suggested in case of C_{60},[1g] with some modifications. Here, we find at high excitation energies a clear dependence of the triplet decay on the concentration, without any noticeable effect of the microwave power. Such a dependence suggests that, in addition to the triplet decay rate, k_T, triplet–triplet annihilation, k_{TT}, should also be taken into account, leading to the following rate equation:

$$-d[^3C_{70}]/dt = k_T[^3C_{70}] + 2k_{TT}[^3C_{70}]^2 \quad (8)$$

which is solved by

$$[^3C_{70}] = k_T[^3C_{70}]_0\{(2k_{TT}[^3C_{70}]_0 + k_T)\exp(k_T t) - 2k_{TT}[^3C_{70}]_0\}^{-1} \quad (9)$$

where $[^3C_{70}]_0$ is the initial concentration of the triplets. Multiplying $M_y(t)$ of eq 6 by eq 9, the simulated curve (Figure 3, top) results in the values $T_1 \approx 280$ ns, $T_2 \approx 100$ ns. It is noteworthy that the fitting is not very sensitive to changes in these values. This value of T_2 is in full agreement with the relaxation time T_2 obtained from the narrow line width ($\sim$0.6 G, from maximum to minimum of the derivative) in the LFM experiment, shown in Figure 3, which corresponds to $\sim$110 ns for T_2.

It should be borne in mind that these relaxation times refer to the decay of the x lines, which according to our motional model are unaffected by the rotation. Using the equations of ref 1c to relate T_1 and T_2 to the corresponding correlation time τ, one finds that the shortest possible T_1 with the ZFS parameters of C_{70} is $T_1 \approx 230$ ns, whereas for C_{60} the shortest time would be $T_1 \approx 63$ ns. Thus, the value of $T_1 \approx 560$ ns found previously for C_{60} is well into the regime in which $T_1 \approx T_2$, as assumed there. In the present case, the relaxation times of C_{70} are quite close to the minimum value of T_1, where T_1 and T_2 are not equal. The values of $T_1 = 280$ ns, $T_2 = 100$ ns used for simulating the kinetics at $T = 213$ K correspond to a correlation time of $\tau \approx 2 \times 10^{-11}$ s, which is related to the x lines. The rotational correlation time of $\tau_R \approx 6 \times 10^{-10}$ s corresponds to the mechanism which brings about the coalescence and broadening of the y, z lines of both triplets. The lines observed experimentally (Figure 3) are the x lines, since the rate of rotation, $1/\tau_R$, is not sufficient for motional narrowing of the y, z lines (for the complete dynamic behavior for a model case, see Figure 4). The shorter correlation time obtained from T_1 and T_2 may be related to pseudorotation, but this requires further study.

Relaxation times of $\sim$200 ns, obtained for the rotating $^3C_{70}$, are too short for observing transient mutations, as indeed confirmed by the experiments. This observation is different from the case of $^3C_{60}$, where the relaxation times were found to be on the order of $\sim$560 ns[1g] and transient nutations accompanied the magnetization behavior in the liquid phase.

Conclusion

The results were shown to be consistent with the presence of a photoexcited triplet state of C_{70} over the full temperature range, from $T = 8$ K (in a glassy solvent) up to $T = 213$ K (in a liquid solvent). This is the same as found for C_{60} over a similar temperature range. Moreover, in both molecules pseudorotation due to Jahn–Teller jumps is found for the low-temperature range, when the solvent is a glass (including the "amorphous" state of toluene). For C_{70}, however, the motion is very slow throughout this temperature range, unlike the strong temperature dependence of the dynamic rate in C_{60}. At high temperatures, when the solvent is a liquid, both molecules exhibit rotational diffusion. As expected due to the lower symmetry of C_{70}, its rotational diffusion is slower than that of C_{60}. An important finding in the case of C_{70} is the evidence for the simultaneous presence of two types of triplets, which are identical in their ZFS parameters and in their initial population ratios of the triplet levels. The differences between them were in their relaxation rates, one type having a faster decay of magnetization (by an order of magnitude) than the other type, and in a small difference in the resonance frequency (a small shift in the g-value). The faster decaying triplet is found to have a stronger intensity than the other one.

Acknowledgment. The fullerenes were prepared by S.M. at Argonne National Laboratory, and we are grateful to Dr. D. Gruen and Dr. L. Stock for their kind assistance. The extremely helpful discussions with Dr. A. Regev are highly acknowledged. This work was partially supported by a DFG grant (Sfb 337). The Farkas Research Center is supported by the Bundesministerium für die Forschung und Technologie and the Minerva Gesellschaft für die Forschung GmbH, FRG. This work is in partial fulfillment of the requirements for a Ph.D. degree (S.M.) at the Hebrew University of Jerusalem. We are grateful to Prof. Hirota for sending us a preprint of his study on the dynamics of $^3C_{70}$ at low temperatures.

Appendix

In the simulations done here for C_{70} it was found that $|D| \approx 3|E|$. The molecule is thus very close to a situation in which $|D| = 3|E|$, and therefore the significance of such a situation will be briefly examined. It is well known that the x, y, and z lines in a triplet EPR spectrum have in the rigid limit the resonance frequencies $\omega_{x(1,2)} = \pm^1/_2(D - 3E)$, $\omega_{y(1,2)} = \pm^1/_2(D + 3E)$, and $\omega_{z(2,1)} = \pm D$, respectively. Thus if $D = 3E$, the two x lines coalesce at $\omega_x = 0$, and also $\omega_{y(1)} = \omega_{z(2)} = D$, $\omega_{y(2)} = \omega_{z(1)} = -D$. If, on the other hand, $D = -3E$, then the two y lines coalesce at $\omega_y = 0$, and then $\omega_{x(1)} = \omega_{z(2)} = D$, $\omega_{x(2)} = \omega_{z(1)} = -D$.

These two cases of degeneracy in the spectrum result from two special physical configurations, as will now be shown. First, suppose that $D = 3E$. In the PAS of the ZFS tensor, the dipolar Hamiltonian can be expressed in terms of the two electronic spins as

$$\mathcal{H}_{ZFS} = \Omega_{xx}s_{1x}s_{2x} + \Omega_{yy}s_{1y}s_{2y} + \Omega_{zz}s_{1z}s_{2z} \quad (A\text{-}1)$$

or, in terms of the total spin operator of the triplet, as

$$\mathcal{H}_{ZFS} = D(S_z^2 - {}^1/_3S^2) + E(S_x^2 - S_y^2) \quad (A\text{-}2)$$

where

$$D = {}^3/_4\Omega_{zz} \qquad E = {}^1/_4(\Omega_{xx} - \Omega_{yy}) \quad (A\text{-}3)$$

It is also known that

$$\Omega_{xx} + \Omega_{yy} + \Omega_{zz} = 0 \quad (A\text{-}4)$$

For the case $D = 3E$ it follows from (A-3) that $\Omega_{zz} = \Omega_{xx} - \Omega_{yy}$, and substituting this in (A-4), one obtains

$$\Omega_{xx} = 0 \quad (A\text{-}5)$$

From the definition of the Ω_{aa} ($a = x$, y, or z): $\Omega_{aa} = \langle\Phi|(r^2 - 3a^2)/r^5|\Phi\rangle$, where $|\Phi\rangle$ is a spatial wave function, $r = (x, y, z)$ is

the vector joining the two electrons, and $r = |r|$ is the distance between them. Therefore, the vanishing of Ω_{aa} is equivalent to

$$\langle\Phi|r^2/r^5|\Phi\rangle = 3\langle\Phi|a^2/r^5|\Phi\rangle \qquad \text{(A-6)}$$

which implies that, on the average, the square of the coordinate a ($=x$, y, or z) is equal to one third of the square of the total distance r. In the present case, x^2 is equal on the average to $^1/_3r^2$. The nonvanishing of Ω_{yy}, Ω_{zz} implies that y^2 and z^2 are not equal on the average to this value. Since $x^2+y^2+z^2=r^2$, the implication is that one of the two coordinates y and z is shorter than x and one is longer than x. If D is positive, so is Ω_{zz}, and then $3z^2$ must be smaller than r^2 on the average. Then z is the short axis and y is the long axis.

If D is negative as in the case of the C_{70}, Ω_{zz} is negative, so $3z^2$ must be larger, on the average, than r^2. Thus, y is the short axis, x has exactly an intermediate length, and z is the long axis. In the opposite case, $D = -3E$, the same considerations lead to $\Omega_{yy} = 0$, from which it follows that y is the axis of intermediate length. For positive D, z is the short axis and x is the long axis, and for negative D, z is the long axis and x is the short axis. In the case of C_{70}, the rotation at high temperatures is about the lines whose frequencies are close to zero. Thus the rotation axis is x if $D = 3E$ or y if $D = -3E$. In both assignments, the rotation is around the direction of the axis of intermediate length, and the rotation causes some random exchange between the long and the short axes.